

New Phytologist

The land plant-specific MIXTA-MYB lineage is implicated in the early evolution of the plant cuticle and the colonization of land.

Journal:	<i>New Phytologist</i>
Manuscript ID	NPH-MS-2020-34196
Manuscript Type:	MS - Regular Manuscript
Date Submitted by the Author:	14-Aug-2020
Complete List of Authors:	Xu, Bo; Institute of Botany Chinese Academy of Sciences, State Key Laboratory of Systematic and Evolutionary Botany; University of Cambridge, Department of Plant Sciences Taylor, Lin; University of Cambridge, Department of Plant Sciences Pucker, Boas; University of Cambridge, Department of Plant Sciences; Bielefeld University, Genetics and Genomics of Plants, Center for Biotechnology; Ruhr-University Bochum Faculty of Biology and Biotechnology, Molecular Genetics and Physiology of Plants Feng, Tao; Wuhan Botanical Garden, CAS Key Laboratory of Plant Germplasm Enhancement and Specialty Agriculture Glover, Beverley; University of Cambridge, Department of Plant Sciences Brockington, Samuel; University of Cambridge, Department of Plant Science
Key Words:	cuticle biosynthesis, evolution, regulatory network, MYB transcription factor, papillate cells, plant terrestrialisation

SCHOLARONE™
Manuscripts

1 **The land plant-specific MIXTA-MYB lineage is implicated in the early evolution**
2 **of the plant cuticle and the colonization of land.**

3

4 **Bo Xu^{1,2}, Lin Taylor², Boas Pucker^{2,3,4}, Tao Feng⁵, Beverley J. Glover^{2*}, Samuel**
5 **F. Brockington^{2*}**

6

7 ¹State Key Laboratory of Systematic and Evolutionary Botany, Institute of Botany,
8 Chinese Academy of Sciences, Beijing, China

9 ²Department of Plant Sciences, University of Cambridge, Cambridge, United
10 Kingdom

11 ³Genetics and Genomics of Plants, Center for Biotechnology, Bielefeld University,
12 Bielefeld, Germany

13 ⁴Molecular Genetics and Physiology of Plants, Faculty of Biology and Biotechnology,
14 Ruhr-University Bochum, Universitätsstraße, Bochum, Germany

15 ⁵CAS Key Laboratory of Plant Germplasm Enhancement and Specialty Agriculture,
16 Wuhan Botanical Garden, Chinese Academy of Sciences, Wuhan, China

17

18 *to whom correspondence should be addressed: sb771@cam.ac.uk, bjg26@cam.ac.uk

19

20 **Abstract**

21

22 ● The evolution of a lipid-based cuticle on aerial plant surfaces protects against
23 dehydration is considered as a fundamental innovation in the colonization of the land
24 by the green plants. However, key evolutionary steps in the early regulation of cuticle
25 synthesis are still poorly understood due to limited studies in early diverging land
26 plant lineages.

27 ● Here, we characterise a land plant specific subgroup 9 R2R3 MYB transcription
28 factor MpSBG9, in the early diverging land plant model *Marchantia polymorpha*, that
29 is homologous to MIXTA genes in vascular plants.

30 ● The MpSBG9 functions as a key regulator of cuticle biosynthesis by preferentially

31 regulating expression of orthologous genes for cutin formation, but not wax
32 biosynthesis genes, implying conserved MYB transcriptional regulation in controlling
33 the cutin biosynthesis pathway as a core genetic network in the common ancestor of
34 all land plants.

35 ● The MpSBG9 homolog also promotes the formation of papillate cells on the
36 adaxial surface of *M. polymorpha*, which is consistent with its canonical role in
37 vascular plants.

38 ● The identification of this conserved role in regulating cuticle synthesis implicates
39 the land-plant specific MIXTA MYB lineage in the early origin and evolution of the
40 cuticle.

41

42 **Key words:** cuticle biosynthesis, evolution, regulatory network, MYB transcription
43 factor, papillate cells, plant terrestrialisation

44

45 **Introduction**

46

47 The colonization of land by plants was a milestone in the evolution of life, which has
48 had a profound impact on global ecosystems (Kenrick & Crane, 1997; Bateman *et al.*,
49 1998). Water availability is one of the major limitations of terrestrial habitats. In
50 plants, the evolutionary transition from aquatic to terrestrial has been accompanied by
51 a suite of adaptations to minimize water loss, facilitating survival and reproduction in
52 a desiccating environment (Corner, 1964; Graham *et al.*, 2000). The plant cuticle is
53 one such adaptation, synthesized and secreted by epidermal cells, and forming a
54 continuous hydrophobic layer at the interface between plant and environment (Raven,
55 1977; Kolattukudy, 1980). The primary function of this waterproof layer is to limit
56 non-stomatal transpiration, providing protection against water loss from plants to the
57 atmosphere (Kolattukudy, 2001; Nawrath, 2006). In addition, cuticle can also serve as
58 a physical barrier against UV radiation, pathogen attack and mechanical damage
59 (Kolattukudy, 2001; Nawrath, 2006). The cuticle is considered to be one of the first of
60 the key innovations necessary to colonize land (Corner, 1964), however, compared to

61 other land plant traits such as stomata (Chater *et al.*, 2016), vasculature (Xu *et al.*,
62 2014; Lu *et al.*, 2020), and roots (Menand *et al.*, 2007; Hetherington & Dolan, 2018),
63 relatively little is known about the genetic pathways underpinning development of the
64 cuticle in early diverging land plants..

65 The cuticle in vascular plants is mainly composed of cutins and waxes (Yeats &
66 Rose, 2013). In most vascular plants, cutins contain a high amount of hydroxylated
67 fatty acids of carbon chain length C16 and C18, with the addition of moieties such as
68 glycerol and phenyl-propanoids (Nawrath, 2006; Li-Beisson *et al.* 2013). These
69 components form a network of cross-linked polyesters, which are covalently linked to
70 polysaccharides on the surface of epidermal cell walls (Fich *et al.*, 2016; Philippe *et*
71 *al.*, 2020). Cutin is insoluble and resistant to degradation, serving as a scaffold for
72 impregnation by waxes, which further contribute to the structure and properties of the
73 cuticle. Cuticular waxes are soluble complex mixtures, consisting of very-long chain
74 fatty acids (VLCFAs) and their derivatives, including ketones, alkanes, primary and
75 secondary alcohols, aldehydes, and wax esters, with mostly carbon chain length
76 ranging from C24 to C40 (Bernard & Joubès, 2013; Yeats & Rose, 2013). Cuticular
77 waxes, depending on their location, are further defined as intra-cuticular waxes, which
78 are impregnated in the cutin matrix, and epi-cuticular waxes, which are assembled as
79 free wax crystals on the surface of the cutin matrix. Cutins and waxes start as long-
80 chain fatty acids in the endoplasmic reticulum but are synthesized by different
81 pathways, and their formation can be roughly divided into three steps: elongation and
82 modification; transport of monomers to the epidermal surface; and subsequent
83 assembly on the outer surface of epidermal cell walls (Bernard & Joubès, 2013; Li-
84 Beisson *et al.* 2013).

85 Recent studies have made considerable progress in understanding the biochemical
86 and genetic basis of cuticle formation in vascular plants (Yeats & Rose, 2013;
87 Domínguez *et al.*, 2017; Fich *et al.*, 2016;). Formation of cutin monomers mainly
88 involves esterification of free fatty acids C16 and C18 with Coenzyme A (CoA) by
89 Long-chain acyl-CoA synthetase (LACS), hydroxylation of acyl-CoA by CYP86A
90 and CYP77A proteins from the cytochrome P450 enzyme family, as well as acyl

91 transfer of activated fatty acids to glycerol by glycerol-3-phosphate acyltransferase
92 (GPAT) to produce mono-acyl glycerol (MAGs) (Wellesen *et al.*, 2001; Schnurr *et*
93 *al.*, 2004; Li *et al.*, 2007; Li-Beisson *et al.*, 2009; Lu *et al.*, 2009; Li-Beisson *et al.*,
94 2013). The cutin monomers are subsequently transported to the cell surface by plasma
95 membrane localized ATP-binding cassette subfamily G (ABCG) transporters (such as
96 ABCG11 and ABCG32) as well as lipid transfer proteins (LTPs), before undergoing
97 polymerization, catalyzed by the GDSL-motif lipase/hydrolase family protein
98 (GDSL) cutin synthase (CUS) (Debono *et al.*, 2009; Bessire *et al.*, 2011; Panikashvili
99 *et al.*, 2011; Yeats *et al.*, 2012; Yeats *et al.*, 2014). The biosynthesis of cuticular
100 waxes constitutes a largely distinct pathway. Sharing the first step with the cutin
101 pathway, the carbon chain of acyl-CoAs is extended to generate a wide range of chain
102 lengths by the Fatty Acid Elongase (FAE) complex consisting of β -ketoacyl-coA
103 synthase (KCS), β -ketoacyl-coa reductase (KCR), 3-hydroxyacyl-coA dehydratase
104 (HCD), and enoyl-coA reductase (ECR) (Millar *et al.*, 1999; Todd *et al.*, 1999; Zheng
105 *et al.*, 2005; Bach *et al.*, 2008; Beaudoin *et al.*, 2009; Kim *et al.*, 2013). The very long
106 chain acyl-CoA precursors then feed into two different pathways. The alcohol
107 forming pathway for the production of primary alcohols and wax esters is catalyzed
108 by ECERIFERUM4 (CER4) and wax synthase/diacylglycerol diacyltransferase1
109 (WSD1) (Rowland *et al.*, 2006; Li *et al.*, 2008). The alkane forming pathway for the
110 production of aldehyde, alkanes, secondary alcohols, and ketones is catalyzed by a
111 complex composed of CER1, CER3, and cytochrome B5 (CYTB5) and further
112 transformed into secondary alcohols and ketones by midchain alkane hydroxylase 1
113 (MAH1), a cytochrome CYP95A enzyme (Aarts *et al.*, 1995; Chen *et al.*, 2003;
114 Bernard *et al.*, 2012). All these wax components are exported to the apoplast by
115 ABCG transporters and LTPs, where they are assembled into cuticular waxes
116 (Debono *et al.*, 2009; Bessire *et al.*, 2011; Panikashvili *et al.*, 2011).

117 Although the majority of genetic studies of the cuticle have taken place in
118 vascular plant systems, a limited number of studies have confirmed the role of genetic
119 orthologs in the synthesis of cuticle in early diverging land plants. Genetic knock-out
120 of an ATP-binding cassette protein from subfamily G (*Pp*ABCG7) from the model

121 moss *Physcomitrella patens* resulted in impaired cuticle deposition and reduced
122 tolerance to dehydration stress (Buda *et al.*, 2013). Disruption of glycerol-3-phosphate
123 acyltransferases (*PpGPAT2* and *PpGPAT4*) in *P. patens* results in growth retardation,
124 reduced cuticle permeability, and reduced tolerance to drought, osmotic and salt stress
125 (Lee *et al.*, 2020). A recent study has identified a member of the cytochrome P450
126 gene family, CYP98, as important in the synthesis of the unusual phenolic-rich
127 composition of the cuticle in *P. patens* (Renault *et al.*, 2017). Finally, orthologues of
128 cutin synthase (*PpCUS1*) from *P. patens* have been shown to perform the requisite
129 polyester synthase activity *in vitro*, although their *in planta* phenotype is untested
130 (Yeats *et al.*, 2014). However, notably all of these studies have taken place in the
131 context of the model moss *P. patens*, and to date, to our knowledge, there has been no
132 genetic insight into cuticle formation in other early diverging model species such as
133 *Marchantia polymorpha*.

134 Although cuticle is present on the epidermis of aerial tissues in all land plant
135 species, the composition, structure, and thickness of cuticle vary greatly among
136 tissues and developmental stages (Lee *et al.*, 2015). Cuticle deposition is regulated in
137 coordination with plant development (Lee *et al.*, 2015; Fich *et al.*, 2016). In flowering
138 plants, the first transcription factor responsible for wax deposition was reported as
139 WAX INDUCER1 (*WIN1*)/SHINE1 (*SHN1*), an AP2/ERF family protein in
140 *Arabidopsis thaliana* (Aharoni *et al.*, 2004; Broun *et al.*, 2004). Further analysis of
141 *WIN1*/*SHN1* also showed that cutin production was increased by overexpression of
142 *WIN1*/*SHN1* (Kannangara *et al.*, 2007). MIXTA, an R2R3 MYB transcription factor
143 from *Antirrhinum majus*, was previously identified as a regulator of the development
144 and formation of the conical shape of petal epidermal cells (Noda *et al.*, 1994).
145 However, in addition to their role in epidermal cell differentiation, recent studies
146 report that proteins related to MIXTA, such as MYB106, control cuticle formation in
147 *A. thaliana* by direct activation of cuticle biosynthesis genes or indirect upregulation
148 via *SHN* genes (Oshima *et al.*, 2013). These findings are supported by studies in
149 *Solanum lycopersicum* where *SISHN3* targets expression of *SIMIXTA*-like protein
150 (Lashbrooke *et al.*, 2015). Additional MYB transcription factors are also implicated in

151 cuticle induction in response to various environmental signals and biotic stresses. For
152 example, MYB94 and MYB96 upregulate cuticular wax formation to enhance
153 tolerance to drought in *A. thaliana*, mediated by ABA signals (Seo *et al.*, 2009; Lee *et*
154 *al.*, 2016). *MYB41* is expressed under osmotic and high salinity conditions, and
155 overexpression of *MYB41* affected the permeability of cuticle in the leaf in *A. thaliana*
156 (Cominelli *et al.*, 2008). Finally, MYB30 has been reported to play a positive role in
157 pathogen response by targeting the VLCFA biosynthesis pathway to influence
158 cuticular wax formation (Raffaele *et al.*, 2008).

159 Studies from vascular plant species have therefore revealed a genetic network
160 regulating cuticle biosynthesis, in which MYB transcription factors play a central
161 role. A handful of orthologous structural components of the downstream genetic
162 pathway have been shown to operate in early-diverging land plants. To date, however,
163 the extent to which a similar transcription factor network controlling cuticle
164 biosynthesis is operating in the earliest diverging land plant lineages is unclear. In the
165 present study, by identification and functional characterization of a MYB
166 transcription factor MpSBG9 protein in the early diverging land plant *Marchantia*
167 *polymorpha*, we show that a core component of the genetic network regulating cuticle
168 biosynthesis and epidermal cell fate is highly conserved across land plants, with a
169 phylogenetic origin that is specific to land plants.

170

171 **Materials and Methods**

172

173 **Plant materials and growth conditions**

174 The 'Cambridge' strain *M. polymorpha* (Pollak *et al.*, 2017) was grown on half
175 strength Gamborg's B5 media with vitamins (pH5.8) containing 1% (w/v) agar at
176 22°C under 16 h-white light and 8 h-dark regime. To induce reproductive organs, *M.*
177 *polymorpha* gemmae were propagated on agar plates for 10 days, and then
178 transplanted into soil at 22°C under 16 h-white light and 8 h-dark conditions in a
179 growth room. After 14 days, the plants were supplemented with far red light (Philips).

180 *Nicotiana. tabacum* was grown at 25°C under 16 h-white light and 8 h-dark
181 conditions in a growth room.

182

183 **Phylogenetic analysis**

184 A previously published MYB gene dataset including all R2R3 MYB genes from *A.*
185 *thaliana*, plus a selection of functionally characterized R2R3 MYB genes from
186 additional plant models (Stracke *et al.*, 2014), was combined with a number of
187 predicted annotated R2R3 MYBs from an early draft of the *M. polymorpha* genome.
188 The dataset comprised 218 sequences, and was translated to amino-acid sequence, and
189 then aligned by MAFFT. The alignment was subject to analysis by FASTtree, with
190 associated calculation of Fasttree SH support values. The immediate Marchantia
191 homolog of the Subgroup9A clade (containing MIXTA and MIXTA-like genes) was
192 identified, with 99% support value.

193

194 **DNA/RNA extraction and cDNA synthesis**

195 About 100mg of fresh thalli from 10-day-old plants was ground frozen using a Tissue
196 Lyer II homogenizer (Qiagen). DNA was extracted using the DNeasy Plant Mini Kit
197 (Qiagen), and RNA contamination was removed by the DNase-Free RNase set
198 (Qiagen). RNA extraction was performed using the RNeasy Plant Mini Kit (Qiagen),
199 and DNA contamination was removed using the TURBO DNA-free Kit (Ambion).
200 cDNA synthesis was carried out using Bioscript Reverse Transcriptase (Bioline
201 Reagents).

202

203 **Microscopy and image analysis**

204 Thallus tips of 28-day-old transgenic Marchantia plants expressing yellow fluorescent
205 protein Venus driven by the promoter of *MpSBG9* were observed using a stereo
206 fluorescence microscope M205 FA (Leica). To detect the expression of Venus at
207 tissue level, the thalli imaged in the previous observation were fixed in 100 mM
208 sodium phosphate buffer (pH7.0) containing 4% paraformaldehyde at 4 °C for 1 hour.
209 The fixed thalli were embedded in 5% (w/v) agar. Sections with 50 µm thickness

210 were made using a vibratome HM340E (Thermo Scientific), and images were
211 acquired using a confocal microscope SP5 (Leica) excited at 515 nm. Imaging of TB
212 stained plants was performed with an optical microscope VHX-5000 (Keyence).
213 Epidermis of thallus tips from WT, *MpSBG9*, and *OX-MpSBG9* (*MpSBG9*
214 overexpressor) lines were observed by a Cryo-SEM EVO HD15 (Zeiss). Size of
215 epidermal cells and number of conical cells were acquired using ImageJ software
216 (<http://rsb.info.nih.gov/ij/>).

217

218 **Toluidine Blue staining and quantification**

219 Thalli of 28-day-old Marchantia plants from wild type (WT), *MpSBG9*, and *OX-*
220 *MpSBG9* lines grown on plate were sampled and stained with Toluidine Blue (TB)
221 solution as described (Tanaka *et al.*, 2004). The plant materials were incubated in
222 staining solution with 0.05% (w/v) of TB (Sigma) at room temperature for 2 min,
223 followed by gentle wash in water three times to remove excessive TB.

224

225 The quantification of TB staining was performed as previously described (Li *et al.*,
226 2016). The stained plants were ground in 400 μ L extraction buffer containing 200
227 mM Tris-HCl (pH8.0), 250mM NaCl, and 25 mM EDTA. After adding 800 μ L
228 ethanol, the samples were vortexed and centrifuged, and the supernatant was
229 examined by a scanning spectrophotometer SpectronicUV1 (Termo Electron Corp.)
230 for absorbance at 630 nm (A_{630}) and 435 nm (A_{435}). Relative absorbance of TB by
231 plants were obtained by calculating the ratio of $A_{630}:A_{435}$.

232

233 **Water loss analysis**

234 Thalli of 21-day-old Marchantia plants from WT, *mpsbg9*, and *OX-MpSBG9* lines
235 grown on plates were detached carefully, and free water on the thalli surface was
236 removed by filter paper. The samples then were transferred to a 9 cm petri-dish
237 without a lid, and weight was monitored every 20 min for up to 4 h by a microbalance
238 at room temperature. Water loss was presented as a percentage of initial fresh weight.

239

240 To test contribution of the *MpSBG9* gene to drought tolerance, 10-day-old thalli
241 grown on plates from WT, *mpsbg9*, and *OX-MpSBG9* lines were transplanted into
242 soil. 14 days later, the lid of the tray was removed and plants were left without
243 watering. After 5 days, the plants were harvested and water content was calculated.

244

245 **Cutin polyester analysis**

246 The thalli of 21-day-old Marchantia plants from WT, *mpsbg9*, and *OX-MpSBG9* lines
247 grown on plates were carefully harvested for cutin polyester analysis as previously
248 described (Lu *et al.*, 2009).

249

250 **Results**

251 **Phylogenetic analysis of MYB transcription factors regulating cuticle**

252 **biosynthesis across land plants**

253

254 MYB domain proteins form a super family, and function as master regulators in a
255 variety of processes in plant development as well as responses to biotic and abiotic
256 stresses (Dubos *et al.*, 2010). Recent studies have revealed a group of R2R3 MYB
257 transcription factors as a key switch controlling cuticle biosynthesis to maintain plant
258 development or mediate responses to drought tolerance and pathogen attack (Aharoni
259 *et al.*, 2004; Raffaele *et al.*, 2008; Seo *et al.*, 2009; Lee *et al.*, 2016). To understand
260 the evolution of the core genetic network underlying land plant cuticle biosynthesis,
261 cuticle-regulating MYB transcription factors in Arabidopsis were used as bait to
262 search against a database of genomes from Phytozome
263 (<https://phytozome.jgi.doe.gov>) and transcriptomes from the 1KP sequencing project
264 (Matasci *et al.*, 2014). Phylogenetic analysis clearly identified a MYB protein
265 Mp0096s0058 homologous to MIXTA (Fig. S1; Bowman *et al.*, 2017), which has
266 previously been implicated in cuticle regulation in vascular plants, in the early
267 diverging land plant model *M. polymorpha*, thereafter referred to *M. polymorpha*
268 subgroup 9 protein (MpSBG9, following the nomenclature of Brockington *et al.*,
269 2013).

270

271 **Expression pattern of the *M. polymorpha* cuticle-related *MpSBG9* Ortholog**

272

273 To better understand the putative function of the *MpSBG9* protein in *M. polymorpha*,
274 a cassette expressing the yellow fluorescent protein Venus fused with a nuclear
275 localization signal (NSL) driven by the *MpSBG9* promoter (*proMpSBG9:Venus-NLS*),
276 containing an ~ 4.0 kb-long genomic fragment upstream of the ATG start codon of
277 the *MpSBG9* gene, was assembled (Fig. S2a; Methods S1). Transgenic *M.*
278 *polymorpha* plants were generated and the expression pattern of the *MpSBG9* gene
279 was investigated by visualization of Venus protein. Expression of Venus was detected
280 in the dorsal surface of thallus, with a higher intensity in the apical notch and
281 surrounding tissues as well as air pore cells (Fig. 1a, b, d). Close observation showed
282 that Venus signals were predominantly restricted to the dorsal and ventral epidermis,
283 filamentous photosynthetic cells within the air chamber, and scales at the ventral
284 surface (Fig. 1c). It was noted that *proMpSBG9* activity was also detected in papillate
285 cells, that resemble conical petal epidermal cells in shape and are widely distributed
286 across the dorsal surface of the growth tip (Fig. 1d). In addition, the Venus signals
287 were also visualized in epidermal cells of both male and female reproductive organs,
288 antheridiophores and archaegoniophores (Fig. 1e, f). In conclusion, the *MpSBG9* gene
289 was expressed in epidermal cells and in epidermal structures such as air pores and
290 projections directly interacting with external environments, as would be expected for
291 a gene potentially involved in cuticle biosynthesis in *M. polymorpha*.

292

293 **Morphologies of *mpsbg9* mutants and *MpSBG9* overexpression lines**

294

295 In order to elucidate *MpSBG9* function in *M. polymorpha*, we produced *MpSBG9* loss
296 of function mutants and transgenic plants overexpressing the *MpSBG9* gene. Two
297 independent *mpsbg9* mutant lines were established using the CRISPR/Cas9-mediated
298 genome editing system (Fig. S2c, d; Methods S1). Frame shift mutations induced by
299 the CRISPR/Cas9 system at the N^o end of the protein introduced a premature stop

300 codon in both lines, and led to complete loss of the R2R3-MYB DNA binding domain
301 of the MpSBG9 protein (Fig. S3). There were no distinguishable differences in
302 growth between either *mpsbg9* mutant line and wild-type plants at a macroscopic
303 level (Fig. S4).

304

305 In addition, transgenic *M. polymorpha* plants overexpressing the *MpSBG9* gene under
306 control of the *M. polymorpha* *Elongation Factor 1 α* promoter (*proEF1 α*) were
307 generated (Fig. S5; Methods S1). Five independent lines were analysed. 10-day-old
308 overexpressor plants with higher abundance of *MpSBG9* transcripts exhibited growth
309 retardation and abnormal thallus development (Fig. S5). In wild-type *M. polymorpha*,
310 air chambers were specified by several rows of cells, and the thallus margin in a
311 smooth shape comprises a few rows of cells. However, in *MpSBG9* overexpression
312 lines, the partitions between each air chamber were increased, and the cells at the
313 thallus margin underwent excessive proliferation, leading to an irregular shape.

314

315 **Essential role for MpSBG9 in *M. polymorpha* cuticle development**

316

317 Cuticle is deposited on the plant surface as a barrier to prevent water loss, and as a
318 result plant surface permeability can be monitored as a proxy for cuticle defects
319 (Tanaka *et al.*, 2004). To test whether cuticle formation was affected in established
320 transgenic plants, a toluidine-blue (TB) staining assay was carried out with 28-day-old
321 *M. polymorpha* thalli from *mpsbg9* mutants and *MpSBG9* overexpressors. The thalli
322 from *MpSBG9* mutants were heavily stained by TB (Fig. 2a). In contrast, only a few
323 dots with slight staining were observed at the base of the thallus lobes in wild-type
324 plants and overexpressors (Fig. 2a). These observations were further supported by
325 measurements of ratio A₆₃₀:A₄₃₅, which represented a relative quantification of TB
326 dye binding to plant samples (Fig. 2b). It also showed that *MpSBG9* overexpressors
327 were much repellent for staining than wide-type plants. To confirm the cuticle defect
328 phenotype, the 28-day-old thalli were gently detached and subjected to a water loss
329 assay as previously described (Aharoni *et al.*, 2004). It was observed that *mpsbg9*

330 mutant thalli lost water much more rapidly through cuticular transpiration than the
331 wild-type plants and *MpSBG9* overexpressors, but there was no difference in water
332 loss rate between *MpSBG9* overexpression lines and wild-type plants (Fig. 2c), even
333 though *MpSBG9* overexpressors were relatively less heavily stained by TB dye (Fig.
334 2b). These results indicated that *MpSBG9* affects permeability of the epidermis in *M.*
335 *polymorpha*, most likely by altering cuticle permeability.

336

337 **Cutin biosynthesis is controlled by *MpSBG9* in *M. polymorpha***

338

339 To further determine whether altered cuticle permeability in *MpSBG9* mutants is due
340 to changes of cuticle composition or total amount, cutin and wax composition of 28-
341 day-old thalli from both *MpSBG9* overexpressors and *MpSBG9* mutants was analysed
342 and measured by gas chromatography mass spectrometry (GC-MS) (Fig. 3). The cutin
343 mainly consists of fatty acids with chain length of even carbon number C16 to C24,
344 and dicarboxylic acids (DCA) and hydroxy fatty acids (HFA) with chain length of
345 C16 and C18. Similar to the cutin constituents in higher land plants, the main
346 constituents of cutin were detected and dominated the cutin matrix of *M. polymorpha*
347 thallus, but the content of these constituents was much lower than that in higher land
348 plants. Overexpression of the *MpSBG9* gene significantly elevated accumulation of all
349 cutin constituents detected in this study, except for C16:0 DCA, which showed a
350 moderate decrease in *MpSBG9* overexpressor plants. By contrast, loss of *MpSBG9*
351 function induced a dramatic decrease of cutin constituents, in particular the contents
352 of C18:1 FA, C18:2 FA, and C18:0 HFA, which declined to nearly an undetectable
353 level. Unlike other constituents, the amount of C16:0 DCA exhibited a strong increase
354 in *mpsbg9* mutants. However, wax was not detected in *M. polymorpha* plants grown
355 under experimental condition in this study. These observations demonstrated that
356 *MpSBG9* plays a key role in regulating cutin biosynthesis in *M. polymorpha*, and that
357 altered cuticle composition may underpin previously discussed changes in
358 permeability

359

360 **The contribution of the cuticle layer to drought tolerance in *M. polymorpha*.**

361

362 A key role of cuticle is to maintain water balance within plants, by preventing
363 excessive non-stomatal water loss. Therefore, plants deprived of cuticle are prone to
364 growth defects, for instance in stature, and leaf shape and size (Aharoni *et al.*, 2004;
365 Oshima *et al.*, 2013). However, no discernible differences between wild-type plants
366 and *mpsbg9* mutants in growth were evident under experimental condition in this
367 study (Fig. S4). Therefore, we tested whether cuticle contributes to drought tolerance
368 in *M. polymorpha*. To do so, 24-day-old plants of wild type, *MpSBG9* over-
369 expressors, and *mpsbg9* mutants grown in soil were exposed to a dehydration
370 condition by removal of the lid from the tray and depletion of watering for 5 days.
371 The drought treatment reduced the whole-plant growth in all treated plants (Fig. 4a).
372 Both *mpsbg9* mutants and *MpSBG9* over-expressors were more sensitive to drought
373 than wild type plants, and exhibited a much more severe wilting phenotype, such as
374 frequent occurrence of brownish tissues at the flank and tip of the thallus, likely due
375 to excessive water loss (Fig. 4a). Compared to the control, the water content in
376 *mpsbg9* mutants and *MpSBG9* over-expressors significantly declined to approximate
377 70%, but water content of wild-type plants was still maintained at approximate 90%,
378 only a 5% decrease (Fig. 4b). These results suggest the importance of *MpSBG9* in
379 regulating water balance and through regulation of the cuticle as a physical barrier
380 against water loss in *M. polymorpha*.

381

382 **Activation of putative cuticle biosynthesis genes by *MpSBG9* in *M. polymorpha***

383

384 To obtain a comprehensive understanding of how the *MpSBG9* protein promotes
385 cuticle biosynthesis in *M. polymorpha*, genome-wide expression analysis was carried
386 out using 10-day-old thallus from plants grown in tissue culture. Ten plants of each
387 line (WT, *MpSBG9*-1, and *OX-MpSBG9*-1) were pooled for each of 3 biological
388 replicates (Methods S2). The expression of 1060 and 965 genes were statistically up-
389 and down-regulated in *OX-MpSBG9* overexpressors and *mpsbg9* mutants respectively

390 (p-value <0.01) (Tables S1, S2). Transcripts of many genes encoding enzymes
391 putatively involved in lipid metabolism were overrepresented among top 50
392 transcripts with dramatically decreased expression in *mpsbg9* mutants, e.g. genes
393 encoding GDSL proteins (Mapoly0003s0312 and Mapoly0012s0165), ABCG
394 transporter (Mapoly0109s0011), and CYP704B subfamily protein
395 (Mapoly0005s0090) (Table S3).

396

397 In this study, we focused on the genes putatively associated with cuticle deposition.
398 The putative genes orthologous to well-known cuticle biosynthesis genes in vascular
399 plants have recently been identified in *M. polymorpha* (Table S4) (Bowman *et al.*,
400 2017). Data analysis showed that the expression profiles in *M. polymorpha* were
401 dramatically changed, with selective up-regulation and down-regulation of cuticle
402 biosynthesis genes in *MpSBG9* overexpressor and *mpsbg9* mutants respectively (Fig.
403 5; Table S5). Further analysis demonstrated that *MpSBG9* regulates a wide range of
404 genes involved in cutin biosynthesis pathway, including orthologs of biosynthesis
405 gene *CYP77A* and *GPATs*, extracellular transporter genes *ABCG11s* and *LTPs*, as
406 well as assembly genes *Cutin Synthase (CUS)* and *Bodyguard (BDG)* (Fig. 5, Table
407 S5). KCS and ECR are two enzymes serving in FAE complex for elongation of acyl-
408 CoAs in wax biosynthesis pathway. The expression of these two genes exhibited a
409 *MpSBG9*-dependent manner, but *MpSBG9* did not appear to regulate the expression
410 of other orthologues of genes known to function in the wax biosynthesis pathway
411 (Fig. 5, Table S5). These results may indicate that *MpSBG9* serves as a key regulator
412 of cuticle formation in *M. polymorpha*, primarily through cutin formation as opposed
413 to wax biosynthesis more generally. This implies the presence of a transcription
414 factor-controlled cutin biosynthesis pathway as a core genetic network for cuticle
415 formation in common ancestors shared by land plants.

416

417 **Functional equivalency between *MpSBG9* and vascular plant MIXTA proteins.**

418

419 Cuticle deposition has been reported to influence development of epidermal cells and

420 their derivatives in vascular plants, and MIXTA family genes were originally
421 identified as regulators of epidermal cell differentiation (Brockington *et al.*, 2013;
422 Javelle *et al.*, 2011; Noda *et al.*, 1994). To investigate whether MpSBG9 is able to
423 affect epidermal cell differentiation in bryophytes, epidermal morphology of 24-day-
424 old *M. polymorpha* thallus was observed using cryo-scanning electron microscopy
425 (Cryo-SEM) (Fig. 6a, b, c; Fig. S6). In *M. polymorpha*, papillae that resemble conical
426 petal cells in shape are dotted across the dorsal surface of the thallus (Fig. 6d; Fig.
427 S6a). These cells are unicellular, and more prolific in the vicinity of the apical notch
428 and growing apex with a frequency of ~6.9 papillae per 100 epidermal cells (Fig. 6d,
429 j). No papillae are found when the thallus is mature (Fig. 6g). Overexpression of
430 *MpSBG9* induced ectopic formation of papillae on the dorsal surface of mature thallus
431 to a frequency of ~9.6 papillae per 100 epidermal cells (Fig. 6e, h, j; Fig. S6b). These
432 papillae were highly similar to those usually found at the growing apex (Fig. 6e).
433 Papillae formation on the dorsal surface of the growth tip showed an approximate 1.8-
434 fold increase in frequency (Fig. 6j). To confirm that MpSBG9 is able to induce
435 papillae formation in *M. polymorpha*, the *mpsbg9* mutants were examined. The
436 development of papillae was highly disrupted, and papillae were rarely found at either
437 growth tip or on mature thallus (Fig. 6f, i; Fig. S6c). The papillae frequency sharply
438 dropped to ~0.1 papillae per 100 epidermal cells (Fig. 6j). In addition, quantitative
439 analysis of epidermal cell size on the dorsal thallus surface revealed that
440 overexpression of the *MpSBG9* gene led to a 1.9-fold and 2.9-fold increase in
441 epidermal cell size at the growth tip and on mature thallus, respectively (Fig. 6k).
442
443 To test the functional conservation between MpSBG9 and MIXTA family proteins in
444 higher land plants, transgenic *Nicotiana tabacum* plants constitutively expressing the
445 *MpSBG9* gene were generated (Fig. S7). No discernible differences were seen in
446 overall morphology between wild-type *N. tabacum* plants and *MpSBG9* expressors. In
447 wild-type *N. tabacum*, the ovary epidermal cells range from flat to gently rounded in
448 shape (Fig. 7c). However, in transgenic *N. tabacum* plants expressing *MpSBG9*, these
449 cells relatively uniformly underwent outgrowth and transformed into conical shapes

450 (Fig. 7d). These results demonstrate that MpSBG9 protein is sufficiently similar to the
451 vascular plant MIXTA orthologues to act as a trans-acting factor for papillate cell
452 gene networks in vascular plants.

453

454 **DISCUSSION**

455

456 Significant research has been undertaken to understand how early plants
457 protected themselves from terrestrial environments, ultimately leading to the
458 colonization of land (Rensing *et al.*, 2008; Banks *et al.*, 2011; Bowman *et al.*, 2017;
459 Nishiyama *et al.*, 2018; Cheng *et al.*, 2019; Zhang *et al.*, 2020; Li *et al.*, 2020; Jiao *et*
460 *al.*, 2020). The evolution of a lipid barrier that controls water loss was essential for the
461 early plants surviving in water-limited environments. Despite recent studies revealing
462 a genetic network underlying cuticle formation in vascular plants, it is still unclear to
463 what extent regulation of this genetic network is conserved in early land plants. In this
464 study, we report that an R2M3-MYB protein MpSBG9, which plays an established
465 role in cuticle regulation in higher plants, also regulates cuticle formation in the early
466 diverging land plant species *M. polymorpha*. Over-expression and mutant lines of
467 MpSBG9 showed altered permeability to aqueous dye, altered rates of water loss in
468 simulated drought experiments, and display altered levels of typical cuticle
469 monomers. Together, these results suggest a conserved role for the MYB MIXTA-like
470 lineage, in the regulation of the cuticle over 450 million years of land plant evolution.

471 Furthermore, through analysis of the gene expression profiles in over-expression
472 versus mutant lines we have revealed a core genetic network regulated by MpSBG9 in
473 controlling cuticle formation in early land plants (Fig. 5). To some extent, this genetic
474 regulatory gene network contains likely orthologues of known genes involved in the
475 cuticle biosynthesis pathway in vascular plants, however, many of the genes and their
476 orthologues have not been functionally analyzed in either vascular plants or early
477 diverging land plants (Table S1). From this putative MIXTA-regulated cuticle gene
478 network, so far, only GPAT (Lee *et al.*, 2020) and ABCG (Buda *et al.*, 2013) have been
479 studied in *P. patens*, with the function of *P. patens* CUS only tested *in vitro* (Yeats *et*

480 *al.*, 2014). However, we identify numerous additional putative homologs of cuticle
481 synthesis genes, which lie within the MpSBG9 transcriptional network, but which are
482 functionally uncharacterised. These data therefore provide a rich source of hypotheses
483 with which to further dissect the conservation of cuticle genetic pathways across land
484 plants, including an understanding of lineage specific diversification and evolution of
485 the cuticle pathway in the early diverging land plant, *M. polymorpha*.

486 Our analyses of the cuticle biochemistry in *M. polymorpha* represent the first
487 comprehensive analysis of chemical composition in this early diverging land plant
488 model. The cutin monomers in *M. polymorpha* consist of DCA (C16-C18), HFA
489 (C16-C18), and fatty acids (C16-C24), and their constituent categories are very
490 similar to those in higher land plants, for example in *A. thaliana* (Fig. 3). Fatty acids
491 are the most abundant constituent, suggesting their critical role in maintaining the
492 cutin matrix of land plants. These data are also consistent with recent observations on
493 *Klebsomidium nitens*, which is a green alga species that is able to grow in both aquatic
494 and terrestrial environments (Hori *et al.*, 2014). It was reported recently that *K. nitens*
495 produces a considerable amount of fatty acids with simple linear carbon chain length
496 from C16 to C18 that attach to cell wall components, when grown on solid medium
497 (Kondo *et al.*, 2016). Intriguingly, the moss *P. patens* at the protonema stage produces
498 a smooth hydrophobic layer of only fatty acids, with C16 as a major constituent, that
499 resembles the secretions of *K. nitens*, while gametophores develop a cutin layer (Lee
500 *et al.*, 2019). Our observations support the idea that fatty acids were already a well-
501 established component in the common ancestors of land plants, with the potential to
502 form a more complex polyester matrix by interaction with other well-known cutin
503 constituents in land plants, including DCA and HFA.

504 Recent studies of cuticle in bryophytes have shown the presence of free waxes on
505 some species of mosses and liverworts (Schönherr & Ziegler, 1975; Cook & Graham,
506 1998; Budke *et al.*, 2011). Using microscopic and histochemical analysis, at least in
507 some mosses, a free wax layer was observed on the surface of gametophores and
508 sporophores. This layer is well developed and resembles the cuticular wax in higher
509 land plants (Busta *et al.*, 2016). For three liverwort species, *M. polymorpha*, *M.*

510 *paleacea*, and *Plagiochasma elongatum*, the waxes were preferentially deposited on
511 air pore cells (Schönherr & Ziegler, 1975). In this study, we were unable to detect free
512 waxes in lab-grown samples of *M. polymorpha* using GC-MS, although we have
513 observed them in wild-grown populations. It has been well documented that the
514 amount and composition of cuticular waxes vary greatly among plant tissues as well
515 as plant species (Jenks & Ashworth, 1999; Bernard & Joubès, 2013). It could be that
516 the amount of wax on the surface of *M. polymorpha* thalli used in lab growth
517 conditions was too low to be detected, as biosynthesis of cuticular wax is greatly
518 affected by growth conditions (Bernard & Joubès, 2013; Yeats & Rose, 2013). Plants
519 generally promote production of cuticular waxes in response to dry environments. The
520 *M. polymorpha* thalli used for chemical analysis of waxes in the present study were
521 grown at a favourable condition with high humidity. Thus, the wax biosynthesis
522 pathway may not be fully activated to accumulate free waxes to a degree that was
523 detectable. Alternatively, these results may imply that protection against water loss in
524 *M. polymorpha* is mainly due to the cutin layer, and also suggest that the hydrophobic
525 lipid layer in *M. polymorpha* is a proto-type cuticle of land plants, in which free
526 waxes play a less substantial role. Further involvement and stronger integration of
527 free waxes via recruitment of the wax biosynthetic pathway may have arisen later in
528 the evolution of the typical land plant cuticle, allowing adaptation of land plants to
529 dehydrating environments. As discussed below, this interpretation may be supported
530 by the analyses of the MpSBG9 expression network, in which orthologues of the
531 known components of the wax biosynthesis pathway are less apparent (Fig. 5).

532 Previous studies in *Arabidopsis* and tomato have shown that the interplay
533 between MIXTA and SHN serves an important role in orchestrating cuticle deposition
534 (Oshima *et al.*, 2013; Lashbrooke *et al.*, 2015). Significantly, in *Arabidopsis*, MIXTA
535 family proteins activate both the cutin and the wax biosynthesis pathways directly, or
536 indirectly through SHN protein to control cuticle formation (Oshima *et al.*, 2013);
537 while in tomato, MIXTA family proteins function downstream of SHN protein to
538 specifically switch on the cutin biosynthesis pathway (Lashbrooke *et al.*, 2015). The
539 regulatory relationship between MIXTA and SHN proteins suggests a complex

540 evolution of the genetic network underlying cuticle formation in vascular plants. In *M.*
541 *polymorpha*, our data show a central role for MpSBG9 in regulating cuticle formation
542 (particularly cutin) but MpSBG9 does not seem to activate the wax biosynthesis
543 pathway or at least not detectably in lab grown systems (Figs 3, 5). Interestingly,
544 genome-wide analysis did not identify SHN orthologues in *M. polymorpha*, although
545 the SHN orthologue appears to have first evolved prior to the divergence of mosses
546 (Bowman *et al.*, 2017). Thus, further functional exploration of SHN orthologues in
547 mosses may provide insights into the genetic changes underlying cuticle evolution
548 and identify the emerging complexity of the interactions between SHN and MIXTA in
549 the control of cuticle formation.

550 In addition to their role in cuticle formation, MIXTA orthologs have been shown
551 to be both positive and negative regulators of trichome and petal conical cell
552 development in a wide range of vascular plant species (Noda *et al.*, 1994; Glover *et*
553 *al.*, 1998; Brockington *et al.*, 2013; Oshima *et al.*, 2013; Shi *et al.*, 2018; Galdon-
554 Armero *et al.*, 2020). The epidermis is a layer of highly differentiated cells on the
555 surface of land plants, playing important roles in interaction with external
556 environments. Epidermal cells have evolved into different shapes with diverse
557 functions contributing to their multiple roles, such as trichomes, which serve a
558 protective function against dehydration and herbivore attacks, and petal conical cells,
559 which generate visual and tactile cues that attract animal pollinators (Serna & Martin,
560 2006; Fattorini & Glover, 2020). We observed that mutation and over-expression of
561 *MpSBG9* led to respective decreases and increases in short papillate protrusions in *M.*
562 *polymorpha* (Figs 6, S6). Furthermore, heterologous expression of *MpSBG9* in
563 tobacco (*N. tabacum*) led to induction of conical cells mainly on the ovary, which is
564 typically the strongest location for conical cell phenotypes in these types of
565 heterologous assay (Fig. 7). The ability of MpSBG9 protein to induce the ectopic
566 formation of papillae in both *M. polymorpha* and tobacco indicates conservation of
567 the pleiotropic properties of MIXTA-like proteins to activate both epidermal
568 outgrowths and cuticle formation. To what extent this pleiotropic activity is
569 developmentally and genetically based, or whether the occurrence of epidermal

570 outgrowths is a consequence of secondary effects of cuticle modification, is an
571 interesting and active research question.

572 In summary, we have identified the first transcriptional regulator of cuticle
573 formation in early diverging bryophytes, and shed light on the gene network it
574 controls, opening multiple research avenues to further dissect cuticle synthesis in
575 early diverging land plants. Our study on *MpSBG9* from the liverwort *M. polymorpha*
576 implies a conserved genetic mechanism underpinning this process in the common
577 ancestor of all land plants, both in control of the cuticle and in epidermal outgrowths.
578 The MYB transcription factor clade containing *MpSBG9* is land-plant specific,
579 therefore its recruitment to specify control of the cuticle may have been an early event
580 in land plant evolution.

581

582 **ACKNOWLEDGMENTS**

583

584 The project was conceived and designed by BX and SFB. BX was responsible for all
585 experiments, and performed all plant transformations, phenotyping, and analysis. BP
586 conducted the RNAseq analysis, TF performed the GCMS analysis. Heterologous
587 transformations were conceived and performed by LT and BJG. BX prepared all the
588 figures and BX and SFB wrote the manuscript, which was edited and approved by all
589 authors. BX thanks the support by Institute of Botany, Chinese Academy of Sciences.
590 SFB would like to acknowledge support of an Independent Research Fellowship from
591 the National Environmental Research Council (NE/K009303/).

592

593 **REFERENCE**

594

595 **Aarts MG, Keijzer CJ, Stiekema WJ, Pereira A.** (1995). Molecular characterization
596 of the CER1 gene of *Arabidopsis* involved in epicuticular wax biosynthesis and
597 pollen fertility. *Plant Cell* 7:2115-27.

598 **Aharoni A, Dixit S, Jetter R, Thoenes E, van Arkel G, Pereira A.** (2004). The
599 SHINE clade of AP2 domain transcription factors activates wax biosynthesis, alters

- 600 cuticle properties, and confers drought tolerance when overexpressed in Arabidopsis.
601 *Plant Cell* **16**:2463-2480.
- 602 **Bach L, Michaelson LV, Haslam R, Bellec Y, Gissot L, Marion J, Da Costa M,**
603 **Boutin JP, Miquel M., Tellier F *et al.*** (2008). The very-long-chain hydroxy fatty
604 acyl-CoA dehydratase PASTICCINO2 is essential and limiting for plant
605 development. *Proceedings of the National Academy Sciences, USA* **105**:14727-
606 14731.
- 607 **Banks JA, Nishiyama T, Hasebe M, Bowman JL, Gribskov M, dePamphilis C,**
608 **Albert VA, Aono N, Aoyama T, Ambrose BA *et al.*** (2011). The Selaginella
609 genome identifies genetic changes associated with the evolution of vascular plants.
610 *Science* **332**:960-963.
- 611 **Bateman RM, Crane PR, DiMichele WA, Kenrick PR, Rowe NP, Speck T, Stein**
612 **EE.** (1998). Early evolution of land plants: phylogeny, physiology, and ecology of
613 the primary terrestrial radiation. *Annual Review of Ecological Systems* **29**: 263-92.
- 614 **Beaudoin F, Wu X, Li F, Haslam RP, Markham JE, Zheng J, Napier JA.** (2009).
615 Functional characterization of the Arabidopsis β -ketoacyl-coenzyme A reductase
616 candidates of the fatty acid elongase. *Plant Physiology* **150**:1174-1191.
- 617 **Bernard A, Domergue F, Pascal S, Jetter R, Renne C, Faure JD, Haslam RP,**
618 **Napier JA, Lessire R, Joubès J.** (2012). Reconstitution of plant alkane biosynthesis
619 in yeast demonstrates that Arabidopsis ECERIFERUM1 and ECERIFERUM3 are
620 core components of a very-long-chain alkane synthesis complex. *Plant Cell* **23**:3106-
621 3118.
- 622 **Bernard A, Joubès J.** (2013). Arabidopsis cuticular waxes: advances in synthesis,
623 export and regulation. *Progress in Lipid Research* **52**: 110-129.
- 624 **Bessire M, Borel S, Fabre G, Carraca L, Efremova V, Yephremov A, Cao Y,**
625 **Jacquat AC, Métraux JP, Nawrath C.** (2011). A member of the PLEIOTROPIC
626 DRUG RESISTANCE family of ATP binding cassette transporters is required for
627 the formation of a functional cuticle in Arabidopsis. *Plant Cell* **23**:1985-1970.
- 628 **Brockington SF, Alvarez-Fernandez R, Landis JB, Alcorn K, Thomas MM,**
629 **Hileman LC, Glover BJ.** (2013). Evolutionary analysis of the MIXTA gene family

- 630 highlights potential targets for the study of cellular differentiation. *Molecular*
631 *Biology and Evolution* **30**:526-540.
- 632 **Broun P, Poindexter P, Osborne E, Jiang CZ, Riechmann JL.** (2004). WIN1, a
633 transcriptional activator of epidermal wax accumulation in Arabidopsis. *Proceedings*
634 *of the National Academy Sciences, USA* **101**:4706-4711.
- 635 **Bowman JL, Kohchi T, Yamato KT, Jenkins J, Shu S, Ishizaki K, Yamaoka S,**
636 **Nishihama R, Nakamura Y, Berger F, Adam C et al.** (2017). Insights into land
637 plant evolution garnered from the *Marchantia polymorpha* genome. *Cell* **171**:287-
638 304.
- 639 **Buda GJ, Barnes WJ, Fich EA, Park S, Yeats TH, Zhao L, Domozych DS, Rose**
640 **JKC.** (2013). An ATP binding cassette transporter is required for cuticular wax
641 deposition and desiccation tolerance in the moss *Physcomitrella patens*. *Plant Cell*
642 **25**:4000-4013.
- 643 **Budke JM, Goffinet B, Jones CS.** (2011). A hundred-year-old question: is the moss
644 calyptra covered by a cuticle? A case study of *Funaria hygrometrica*. *Annals of*
645 *Botany* **107**:1279-1286.
- 646 **Busta L, Budke, JM, Jetter R.** (2016). The moss *Funaria hygrometrica* has cuticular
647 wax similar to vascular plants, with distinct composition on leafy gametophyte,
648 calyptra and sporophyte capsule surfaces. *Annals of Botany* **118**:511-522.
- 649 **Chater CC, Caine RS, Tomek M, Wallace S, Kamisugi Y, Cuming AC, Lang D,**
650 **MacAlister CA, Casson S, Bergmann DC et al.** (2016). Origin and function of
651 stomata in the moss *Physcomitrella patens*. *Nature Plants* **2**:16179.
- 652 **Chen X, Goodwin SM, Boroff VL, Liu X, Jenks MA.** (2003). Cloning and
653 characterization of the WAX2 gene of Arabidopsis involved in cuticle membrane
654 and wax production. *Plant Cell* **15**:1170-1185.
- 655 **Cheng S, Xian W, Fu Y, Marin B, Keller J, Wu T, Sun W, Li X, Xu Y, Zhang Y et**
656 **al.** (2019). Genomes of subaerial Zygnematophyceae provide insights into land plant
657 evolution. *Cell* **179**:1057-1067.
- 658 **Cominelli E, Sala T, Calvi D, Gusmaroli G, Tonelli C.** (2008). Over-expression of
659 the Arabidopsis AtMYB41 gene alters cell expansion and leaf surface permeability.

- 660 *Plant Journal* **53**:53-64.
- 661 **Cook ME, Graham LE.** (1998). Structural similarities between surface layers of
662 selected Charophyceam algae and bryophytes and the cuticles of vascular plants.
663 *International Journal of Plant Sciences* **159**:780-787.
- 664 **Corner EJH.** (1981) *The Life of Plants*. Chicago, USA: University of Chicago Press.
- 665 **DeBono A, Yeats TH, Rose JK, Bird D, Jetter R, Kunst L, Samuels L.** (2009).
666 Arabidopsis LTPG is a glycosylphosphatidylinositol-anchored lipid transfer protein
667 required for export of lipids to the plant surface. *Plant Cell* **21**:1230-1238.
- 668 **Delmans M, Pollak B, Haseloff J.** (2017). MarpoDB: an open registry for *Marchantia*
669 *polymorpha* genetic parts. *Plant and Cell Physiology* **58**:e5.
- 670 **Dobin A, Davis CA, Schlesinger F, Drenkow J, Zaleski C, Jha S, Batut P, Chaisson**
671 **M, Gingeras TR.** (2013). STAR: ultrafast universal RNA-seq aligner.
672 *Bioinformatics* **29**:15-21.
- 673 **Dubos C, Stracke R, Grotewold E, Weisshaar B, Martin C, Lepiniec L.** (2010).
674 MYB transcription factors in Arabidopsis. *Trends in Plant Science*. **15**:573-581.
- 675 **Domínguez E, Heredia-Guerrero JA, and Heredia A.** (2017). The plant cuticle: old
676 challenges, new perspectives. *Journal of Experimental Botany* **68**:5251-5255.
- 677 **Fich EA, Segerson NA, Rose JKC.** (2016). The plant polyester cutin: biosynthesis,
678 structure, and biological roles. *Annual Review of Plant Biology* **67**:207-233.
- 679 **Fattorini R, Glover BJ.** (2020). Molecular mechanisms of pollination biology. *Annual*
680 *Review of Plant Biology* **71**:21.1-21.29.
- 681 **Galdon-Armero J, Arce-Rodriguez L, Downie M, Li J, Martin C.** (2020). A
682 scanning electron micrograph-based resource for identification of loci involved in
683 epidermal development in tomato: elucidation of a new function for the Mixta-like
684 transcription factor in leaves. *Plant Cell* **32**:1414-1433.
- 685 **Gibson DG, Young L, Chuang RY, Venter JC, Hutchison CA, Smith HO.** (2009).
686 Enzymatic assembly of DNA molecules up to several hundred kilobases. *Nature*
687 *Methods* **6**:343-345.
- 688 **Glover BJ, Perez-Rodriguez M, Martin C.** (1998). Development of several epidermal
689 cell types can be specified by the same MYB-related plant transcription factor.

- 690 *Development* **125**:3497-3508.
- 691 **Graham LE, Cook ME, Busse JS.** (2000). The origin of plants: body plan changes
692 contributing to a major evolutionary radiation. *Proceedings of the National Academy*
693 *Sciences, USA* **97**: 4535-4540.
- 694 **Haak M, Vinke S, Keller W, Droste J, Rückert C, Kalinowski J, Pucker B.** (2018).
695 High quality *de novo* transcriptome assembly of *Croton tiglium*. *Frontiers in*
696 *Molecular Biosciences* **6**:62.
- 697 **Hellens RP, Edwards EA, Leyland NR, Bean S, Mullineaux PM.** (2000). pGreen: a
698 versatile and flexible binary Ti vector for Agrobacterium-mediated plant
699 transformation. *Plant Molecular Biology* **42**:819-832.
- 700 **Hetherington AJ, Dolan L.** (2018). Stepwise and independent origins of roots among
701 land plants. *Nature* **561**: 235-238.
- 702 **Hori K, Maruyama F, Fujisawa T, Togashi T, Yamamoto N, Seo M, Sato S, Yamada,**
703 **T, Mori H, Tajima N et al.** (2014). Klesormidium flaccidum genome reveals
704 primary factors for plant terrestrial adaptation. *Nature Communication* **5**:3978
- 705 **Horsch RB, Fry JE, Hoffman NL, Eichholtz D, Robergs SG, Fraley RT.** (1985). A
706 simple and general method for transferring genes into plants. *Science* **227**:1229-1231.
- 707 **Javelle M, Vernoud V, Rogowsky PM, Ingram GC.** (2011). The formation and
708 functions of a fundamental plant tissue. *New Phytologist* **189**:17-39.
- 709 **Jiao I, Sørensen I, Sun X, Sun H, Behar H, Alseekh S, Philippe G, Lopez KP, Sun**
710 **L, Reed R et al.** (2020). The penium margaritaceum genome: Hallmarks of the
711 origins of land plants. *Cell* **181**:1097-1111.
- 712 **Jenks MA, Ashworth EN.** (1999). Plant epicuticular waxes: function, production and
713 genetics. *Horticultural Reviews* **23**:1-68.
- 714 **Kannangara R, Branigan C, Liu Y, Penfield T, Rao V, Mouille G, Höfte H, Pauly**
715 **M, Riechmann JL, Broun P.** (2007). The transcription factor WIN1/SHN1
716 regulates cutin biosynthesis in *Arabidopsis thaliana*. *Plant Cell* **19**:1278-1294.
- 717 **Kenrick P, Crane PR.** (1997). The origin and early evolution of plants on land.
718 *Nature* **389**: 33-39.
- 719 **Kim J, Jung JH, Lee SB, Go YS, Kim HJ, Cahoon R, Markham JE, Cahoon EB,**

- 720 **Suh MC.** (2013). Arabidopsis 3-ketoacyl-coenzyme A synthase9 is involved in the
721 synthesis of tetracosanoic acids as precursors of cuticular waxes, suberins,
722 sphingolipids, and phospholipids. *Plant Physiology* **162**:567-580.
- 723 **Kolattukudy PE.** (1980). Biopolyester membranes of plants: cutin and suberin.
724 *Science* **208**: 990-1000.
- 725 **Kolattukudy PE.** (2001). Polyesters in higher plants. *Advances in Biochemical*
726 *Engineering Biotechnology* **71**:1-49.
- 727 **Kondo S, Hori K, Sasaki-Sekimoto Y, Kobayashi A, Kato T, Yuno-Ohta N,**
728 **Nobusawa T, Ohtaka K, Shimojima M, Ohta H.** (2016). Primitive extracellular
729 lipid components on the surface of the charophytic alga *Klebsormidium flaccidum*
730 and their possible biosynthetic pathways as deduced from the genome sequence.
731 *Frontier in Plant Science* **7**:952.
- 732 **Lashbrooke J, Adato A, Lotan O, Alkan N, Tsimbalist T, Rechav K, Fernandex-**
733 **Moreno J, Widemann E, Grausem B, Pinot F et al.** (2015). The tomato MIXTA-
734 like transcription factor coordinates fruit epidermis conical cell development and
735 cuticular lipid biosynthesis and assembly. *Plant Physiology* **169**:2553-2571.
- 736 **Lee SB, Suh MC.** (2015). Advances in the understanding of cuticular waxes in
737 Arabidopsis thaliana and crop species. *Plant Cell Reports* **34**:557-572.
- 738 **Lee SB, Kim HU, Suh MC.** (2016). MYB94 and MYB96 additively activate cuticular
739 wax biosynthesis in Arabidopsis. *Plant and Cell Physiology* **0**:1-12.
- 740 **Lee SB, Yang SU, Pandey G, Kim MS, Hyoungh S, Choi D, Shin JS, Suh MC.** (2020).
741 Occurrence of land-plant-specific glycerol-3-phosphate acyltransferases is essential
742 for cuticle formation and gametophore development in *Physcomitrella patens*. *New*
743 *Phytologist* **225**:2468-2483.
- 744 **Li F, Wu X, Lam P, Bird B, Zheng H, Samuels L, Jetter R, Kunst L.** (2008).
745 Identification of the wax ester synthase/acyl-coenzyme A: diacylglycerol
746 acyltransferase WSD1 required for stem wax ester biosynthesis in Arabidopsis. *Plant*
747 *Physiology* **148**:97-107.
- 748 **Li FW, Nishiyama T, Waller M, Frangedakis E, Keller J, Li Z, Fernandez-Pozo**
749 **N, Barker MS, Bennett T, Blazquez MA et al.** (2020). Anthoceros genomes

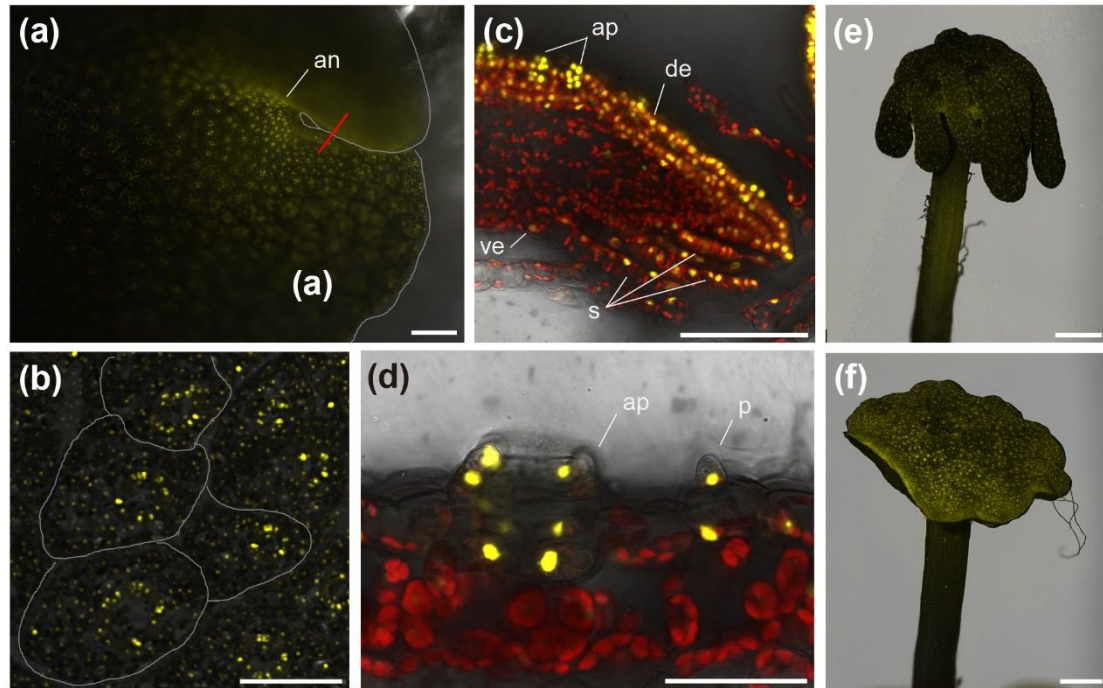
- 750 illuminate the origin of land plants and the unique biology of horworts. *Nature Plants*
751 **6**:259-272.
- 752 **Li S, Wang X, He S, Li J, Huang Q, Imaizumi T, Qu L, Qin G, Qu LJ, Gu H.**
753 (2016). CFLAP1 and CFLAP2 are two bHLH transcription factors participating in
754 synergistic regulation of AtCFL1-mediated cuticle development in Arabidopsis.
755 *PLoS Genetics* **12**:e1005744.
- 756 **Li Y, Beisson F, Koo AJ, Molina I, Pollard M, Ohlrogge J.** (2007). Identification of
757 acyltransferases required for cutin biosynthesis and production of cutin with suberin-
758 like monomers. *Proceedings of the National Academy Sciences, USA* **104**:18339-
759 18344.
- 760 **Liao Y, Smyth GK, Shi W.** (2014). featureCounts: an efficient general purpose
761 program for assigning sequence reads to genomic features. *Bioinformatics* **30**:923-
762 930.
- 763 **Li-Besson Y, Pollard M, Sauveplane V, Pinot F, Ohlrogge J, Beisson F.** (2009).
764 Nanoridges that characterize the surface morphology of flowers require the synthesis
765 of cutin polyester. *Proceedings of the National Academy Sciences, USA* **106**:22008-
766 22013.
- 767 **Li-Beisson Y, Shorrosh B, Beisson F, Andersson M, Arondel V, Bates P, Baud S,**
768 **Bird D, Debono A, Durrett T et al.** (2013). Acyl-lipid metabolism. *The Arabidopsis*
769 *Book/American Society of Plant Biologist* **11**: e0161.
- 770 **Love M, Huber W, Anders S.** (2014). Moderated estimation of fold change and
771 dispersion for RNA-seq data with DESeq2. *Genome Biology* **15**:550.
- 772 **Lu K-J, van't Wout Hofland N, Mor E, Mutte S, Abrahams P, Kato H, Vandepoele**
773 **K, Weijers D, De Rybel B.** (2020). Evolution of vascular plants through
774 redeployment of ancient developmental regulators. *Proceedings of the National*
775 *Academy Sciences, USA* **117**:733-740.
- 776 **Lu S, Song T, Kosma DK, Parsons EP, Rowland O, Jenks MA.** (2009). Arabidopsis
777 *CER8* encodes LONG-CHAIN ACYL-COA SYNTHETASE 1 (LACS1) that has
778 overlapping functions with LACS2 in plant wax and cutin synthesis. *Plant Journal*
779 **59**:553-64.

- 780 **Menand B, Yi K, Jouannic S, Hoffmann L, Ryan E, Linstead P, Schaefer DG,**
781 **Dolan L.** (2007). An ancient mechanism controls the development of cells with a
782 rooting function in land plants. *Science* **316**:1477-1480.
- 783 **Matasci N, Hung L-H, Yan Z, Carpenter EJ, Wichett NJ, Mirarab S, Nguyen N,**
784 **Warnow T, Ayyampalayam S, Barker M et al.** (2014). Data access for the 1,000
785 Plants (1KP) project. *GigaScience* **3**:17
- 786 **Millar AA, Clemens S, Zachgo S, Giblin EM, Taylor DC, Kunst L.** (1999). CUT1,
787 an Arabidopsis gene required for cuticular wax biosynthesis and pollen fertility,
788 encodes a very-long-chain fatty acid condensing enzyme. *Plant Cell* **11**:825-38.
- 789 **Nawrath C.** (2006). Unraveling the complex network of cuticular structure and
790 function. *Current Opinion in Plant Biology* **9**: 281-287.
- 791 **Nishiyama T, Sakayama H, de Vries J, Buschmann H, Saint-Marcoux D, Ullrich**
792 **KK, Haas FB, Vanderstraeten L, Becher D, Lang D et al.** (2018). The chara
793 genome: Secondary complexity and implications for plant terrestrialization. *Cell*
794 **174**:448-464.
- 795 **Noda K, Glover BJ, Linstead P, Martin C.** (1994). Flower colour intensity depends
796 on specialized cell shape controlled by an MYB-related transcription factor. *Nature*
797 **369**:661-664.
- 798 **Oshima Y, Shikata M, Koyama T, Ohtsubo N, Mitsuda N, Ohme-Takagi Y.** (2013).
799 MIXTA-like transcription factors and WAX INDUCER1/SHINE1 coordinately
800 regulate cuticle development in Arabidopsis and *Torenia fournieri*. *Plant Cell*
801 **25**:1609-1624.
- 802 **Panikashvili D, Shi JX, Schreiber L, Aharoni A.** (2011). The Arabidopsis ABCG13
803 transporter is required for flower cuticle secretion and patterning of the petal
804 epidermis. *New Phytologist* **190**:113-124.
- 805 **Philippe G, Sørensen I, Jiao C, Sun X, Fei Z, Domozych DS, Rose JKC.** (2020).
806 Cutin and suberin: assembly and origins of specialized lipidic cell wall scaffolds.
807 *Current Opinion in Plant Biology* **55**:11-20.
- 808 **Pollak B, Delmans M, Haseloff J.** (2017). Analysis of Cambridge isolates of
809 *Marchantia polymorpha*. In: Bowman JL, Kohchi T, Yamato KT, Jenkins J, Shu S,

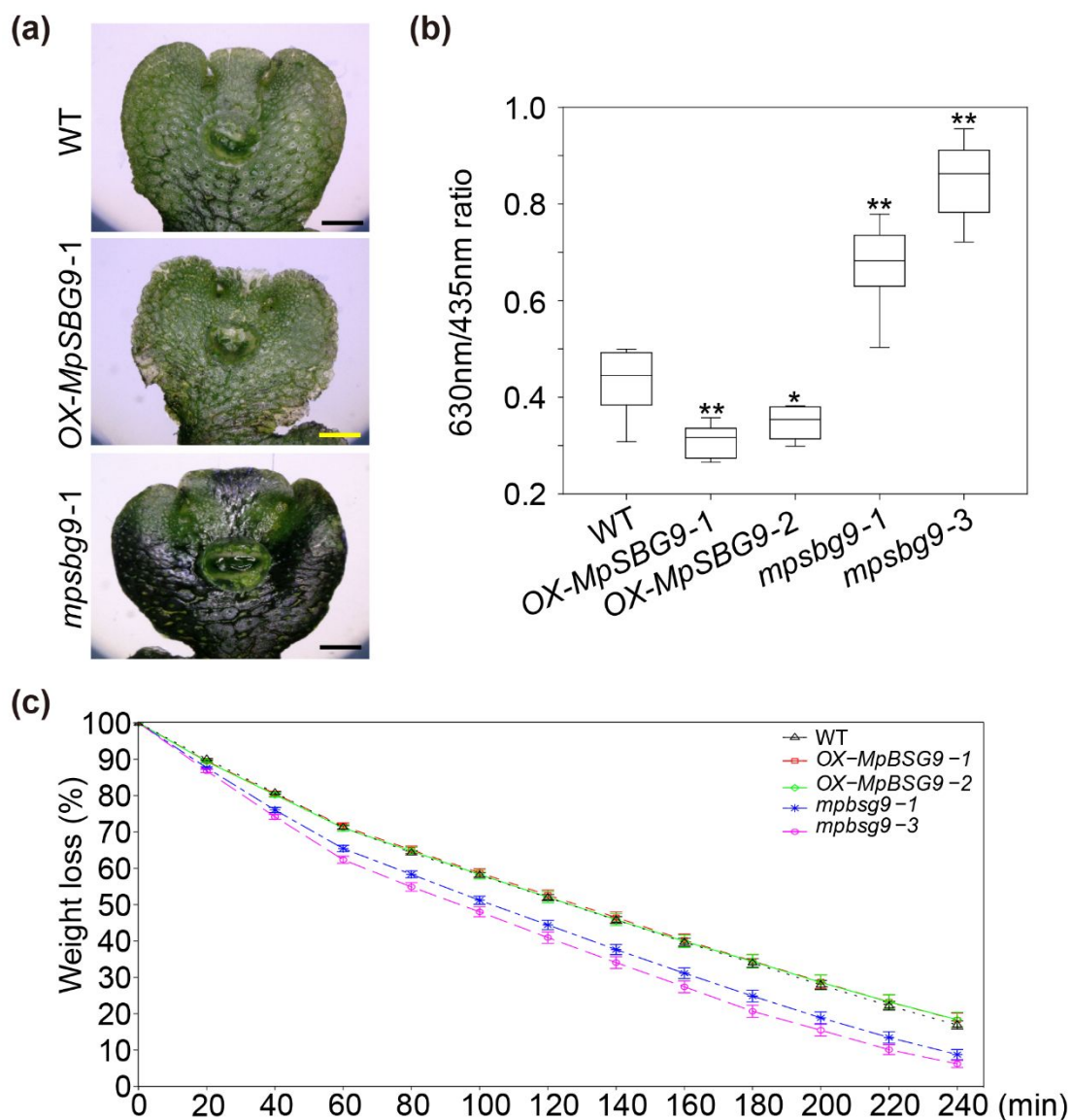
- 810 Ishizaki K, Yamaoka S, Nishihama R, Nakamura Y, Berger F, Adam C *et al.* Insights
811 into land plant evolution garnered from the *Marchantia polymorpha* genome. *Cell*
812 **171**:287-304.
- 813 **Raffaele S, Vaillau F, Léger A, Joubès J, Miersch O, Huard C, Blée E, Mongrand**
814 **S, Domergue F, Roby D.** (2008). A MYB transcription factor regulates very-long-
815 chain fatty acid biosynthesis for activation of the hypersensitive cell death response
816 in Arabidopsis. *Plant Cell* **20**:752-767.
- 817 **Raven JA.** 1977. The evolution of vascular land plants in relation to supracellular
818 transport processes. *Advances in Botanical Research* **5**:153-219.
- 819 **Renault H, Alber A, Nelly AH, Lopes AB, Fich EA, Kriegshauser L, Wiedemann**
820 **G, Ullmann P, Herrgott L, Erhardt M et al.** (2017). A phenol-enriched cuticle is
821 ancestral to lignin evolution in land plants. *Nature Communication* **8**:14713.
- 822 **Resing SA, Lang D, Zimmer AD, Terry A, Salamov A, Shapiro H, Nishiyama T,**
823 **Perroud PF, Lindquist EA, Kamisugi Y et al.** (2008). The Physcomitrella
824 genome reveals evolutionary insights into the conquest of land by plants. *Science*
825 **319**:64-69.
- 826 **Rowland O, Zheng H, Hepworth SR, Lam P, Jetter R, Kunst L.** (2006). CER4
827 encodes an alcohol-forming fatty acyl-coenzyme A reductase involved in cuticular
828 wax production in Arabidopsis. *Plant Physiology* **142**:866-877.
- 829 **Schnurr J, Shockey J, Browse J.** (2004). The acyl-CoA synthetase encoded by *LACS2*
830 is essential for normal cuticle development in Arabidopsis. *Plant Cell* **16**:629-42.
- 831 **Schönher J, Ziegler H.** (1975). Hydrophobic cuticular ledges prevent water entering
832 the air pores of liverwort thalli. *Planta* **124**:51-60.
- 833 **Seo PJ, Xiang F, Qiao M, Park JY, Lee YH, Park WJ, Park CM.** (2009). The
834 MYB96 transcription factor mediates abscisic acid signaling during drought stress
835 response in Arabidopsis. *Plant Physiology* **151**:275-289.
- 836 **Serna L, Martin C.** (2006). Trichomes: different regulatory networks lead to
837 convergent structures. *Trends in Plant Science* **11**:274-280.
- 838 **Shi P, Fu X, Shen Q, Liu M, Pan Q, Tang Y, Jiang W, Lv Z, Yan T, Ma Y et al.**
839 (2018). The roles of AaMIXTA1 in regulating the initiation of glandular trichomes

- 840 and cuticle biosynthesis in *Artemisia annua*. *New Phytologist* **217**:261-276.
- 841 **Stracke R, Holtgräwe D, Schneider J, Pucker B, Sørensen TR, Weisshaar B.**
842 (2014). Genome-wide identification and characterization of R2R3-MYB genes in
843 sugar beet (*Beta vulgaris*). *BMC Plant Biology* **14**:249.
- 844 **Sugano SS, Shirakawa M, Takagi J, Matsuda Y, Shimada T, Hara-Nishima I,**
845 **Kochi T.** (2014). CRISPR/Cas9-mediated targeted mutagenesis in the liverwort
846 *Marchantia polymorpha* L. *Plant and Cell Physiology* **55**:475-481.
- 847 **Tanaka T, Tanaka H, Machida C, Watanabe M, Machida Y.** (2004) A new method
848 for rapid visualization of defects in leaf cuticle reveals five intrinsic patterns of
849 surface defects in Arabidopsis. *Plant Journal* **37**:139-146.
- 850 **Todd J, Post-Beittenmiller D, Jaworski JG.** (1999). *KCSI* encodes a fatty acid
851 elongase 3-ketoacyl-CoA synthase affecting wax biosynthesis in Arabidopsis
852 thaliana. *Plant Journal* **17**:119-130.
- 853 **Jiao C, Sørensen I, Sun X, Sun H, Behar H, Alseekh S, Philippe G, Lopez KP, Sun**
854 **L, Reed R et al.** (2020). The Penium Margaritaceum genome: Hallmarks of the
855 origins of land plants. *Cell* **181**:1097-1111.
- 856 **Wellesen K, Durst F, Pinot F, Benveniste I, Nettekheim K, Wisman E, Steiner-**
857 **Lange S, Saedler H, Yephremov A.** (2001). Functional analysis of the LACERATA
858 gene of Arabidopsis provides evidence for different roles of fatty acid omega-
859 hydroxylation in development. *Proceedings of the National Academy Sciences, USA*
860 **98**:9694-9699.
- 861 **Xu B, Ohtani M, Yamaguchi M, Toyooka K, Wakazaki M, Sato M, Kubo M,**
862 **Nakano Y, Sano R, Hiwatashi Y et al.** (2014). Contribution of NAC transcription
863 factors to plant adaptation to land. *Science* **343**:1505-1508.
- 864 **Yeats TH, Huang W, Chatterjee S, Viart HMF, Clausen MH, Stark RE, Rose JK.**
865 (2014). Tomato Cutin Deficient 1 (CD1) and putative orthologs comprise an ancient
866 family of cutin synthase-like (CUS) proteins that are conserved among land plants.
867 *Plant Journal* **77**:667-675.
- 868 **Yeats TH, Martin LB, Viart HM, Isaacson T, He Y, Zhao L, Matas AJ, Buda GJ,**

- 869 **Domozych DS, Clausen MH, Rose JK.** (2012). The identification of cutin synthase:
870 formation of the plant polyester cutin. *Nature Chemical Biology* **8**:609-611.
- 871 **Yeats TH, Rose JKC.** (2013). The formation and function of plant cuticles. *Plant*
872 *Physiology* **160**: 5-20.
- 873 **Zhang J, Fu XX, Li RO, Zhao X, Liu Y, Li MH, Zwaenepoel A, Ma H, Goffinet B,**
874 **Guan YL *et al.*** (2020). The hornwort genome and early land plant evolution. *Nature*
875 *Plants* **6**:107-118.
- 876 **Zheng H, Rowland O, Kunst L.** (2005). Disruptions of the Arabidopsis enoyl-CoA
877 reductase gene reveal an essential role for very-long-chain fatty acid synthesis in the
878 cell expansion during plant morphogenesis. *Plant Cell* **17**:1467-1481.



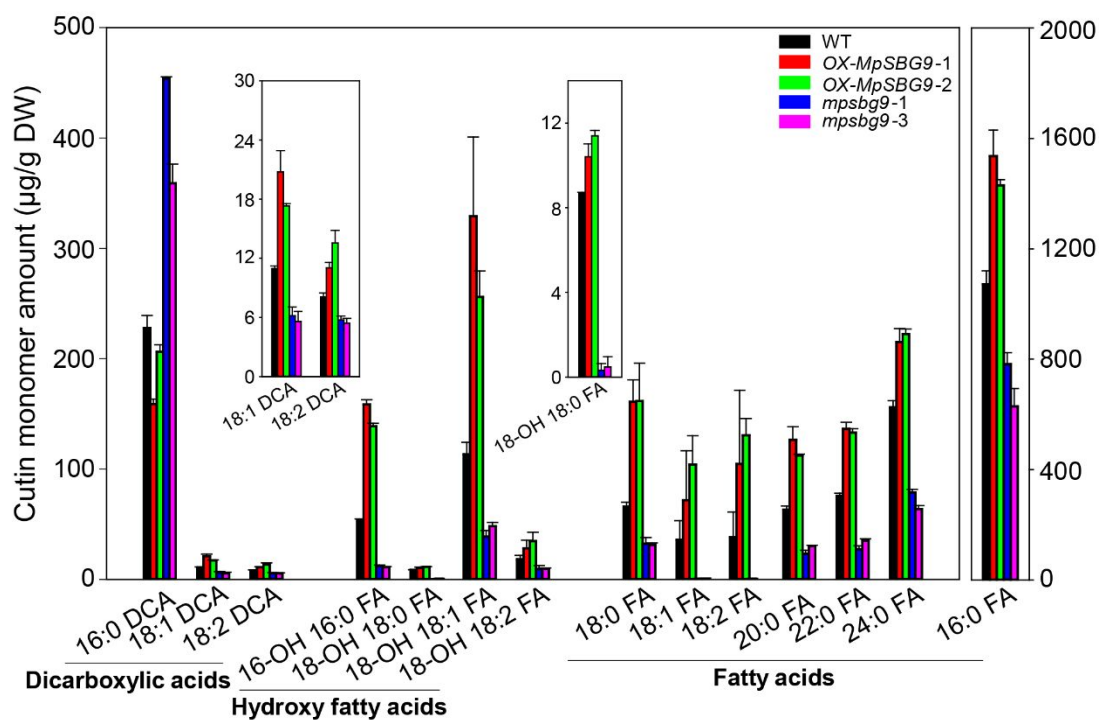
879 **Fig. 1** Expression of *MpSBG9* in *M. polymorpha*. Visualisation of Venus expression
 880 in vegetative tissues (a-d) and reproductive organs (e-f) from representative
 881 *proMpSBG9:Venus-NLS* lines. (a) Dorsal view of a 28-day-old thallus tip grown on
 882 half strength Gamborg's B5. Thallus tip is outlined in gray. (b) Close-up view of
 883 thallus surface in (a). Air chambers are indicated by gray lines. (c-d) Transverse
 884 sections of the developing region indicated by the red line in (a). an, apical notch; ap,
 885 air pore; de, dorsal epidermis; ve, ventral epidermis; s, scale; p, papilla. (e)
 886 Antheridiophore. (f) Archaeogoniophore. Scale bars, 1 mm in (a), (e), and (f); 200 μ m
 887 in (b); 100 μ m in (c); and 50 μ m in (d).



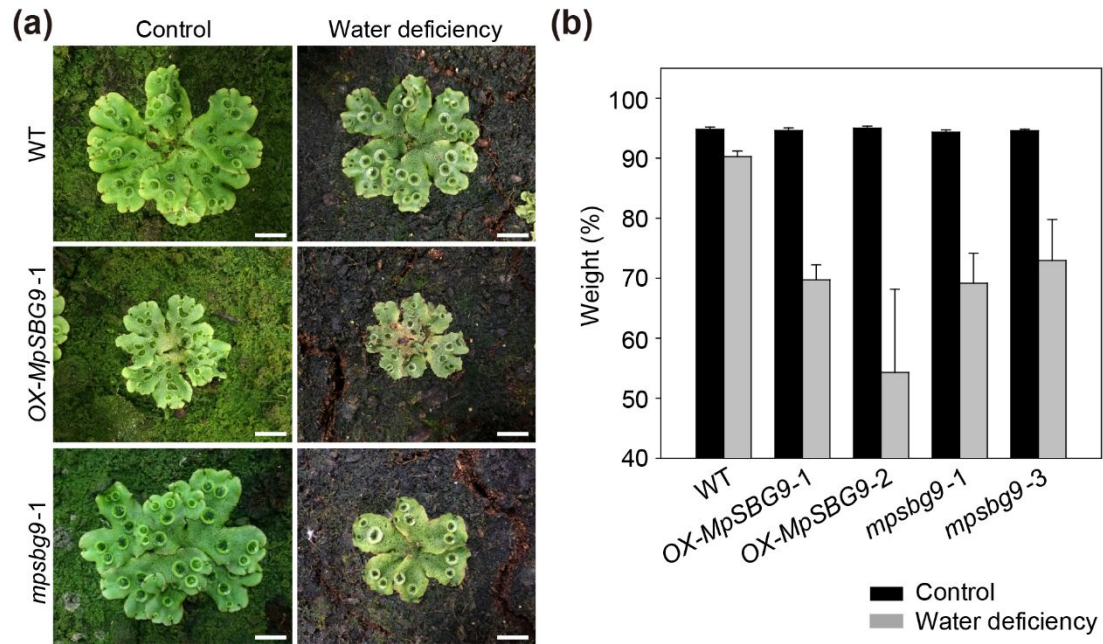
888 **Fig. 2** Surface permeability of wild type (WT), *OX-MpSBG9*, and *mpsbg9* *M.*
 889 *polymorpha* plants. (a) 28-day-old thalli grown on half strength Gamborg's B5 plate
 890 stained by Toluidine blue solution (0.05%, w/v). Top, WT; middle, *OX-MpSBG9* line
 891 1; bottom, *mpsbg9* mutant line 1. Scale bars, 2 mm. (b) Quantification of Toluidine
 892 blue staining. Each measurement represents mean \pm standard error (SE) of 8
 893 biological replicates. The thalli from 3 plants were harvested for each replicate. * $P <$
 894 0.05 and ** $P <$ 0.01 (Welch's *t* test). All comparisons were performed against WT.
 895 (c) Water loss assay. 28-day-old thalli grown on half strength Gamborg's B5 were
 896 carefully detached and placed in a weighting boat in air at room temperature. The
 897 weight was monitored every 20 min up to 4 h. Water loss was presented as a ratio to
 898 fresh weight at the start. Each measurement represents mean \pm standard error (SE) of

899 four biological replicates. The thalli from at least 3 plants were harvested for each
900 replicate.

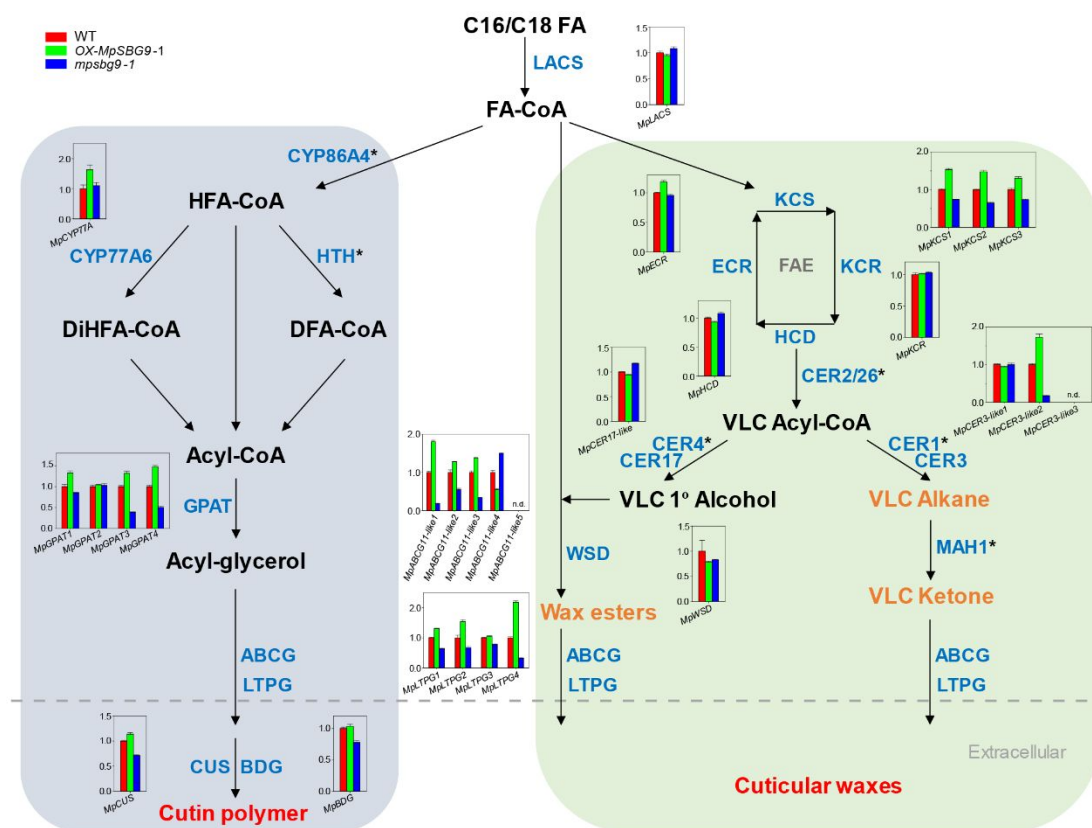
For Peer Review



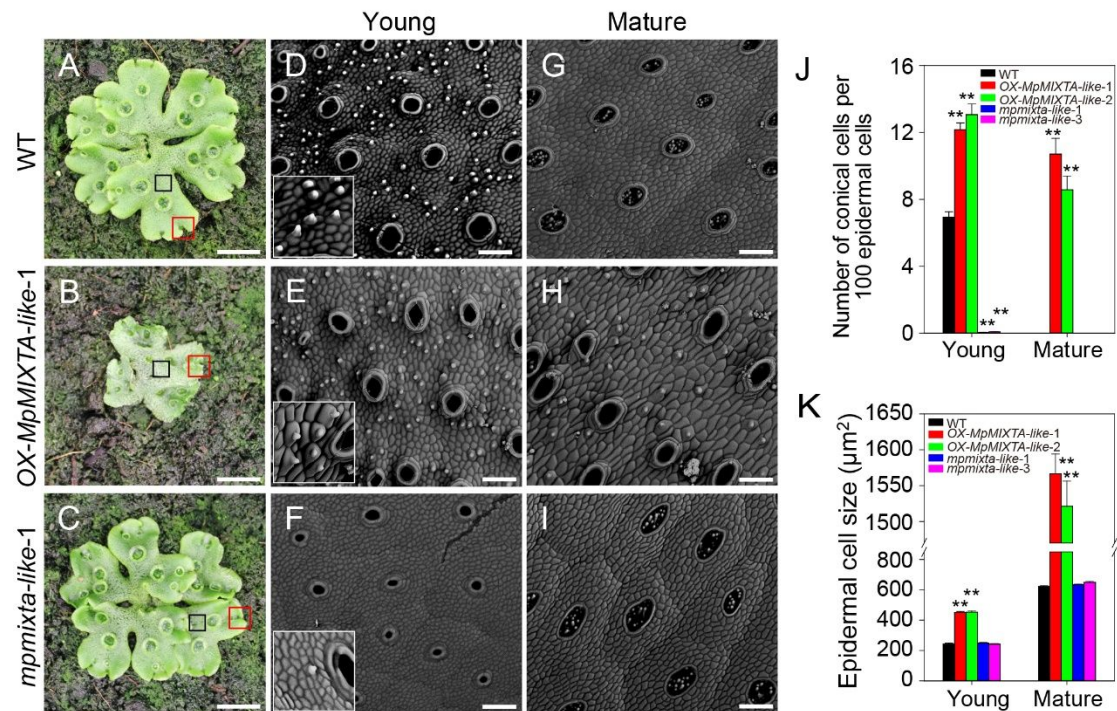
901 **Fig. 3** Cutin polyester compositions and amounts in thalli of WT, *OX-MpSBG9*, and
 902 *mpsbg9* *M. polymorpha* plants. 28-day-old thalli grown on half strength Gamborg's
 903 B5 plate were used for examination. Each measurement represents mean \pm SE of three
 904 biological replicates. The thalli from at least 5 plants were harvested for each
 905 replicate.



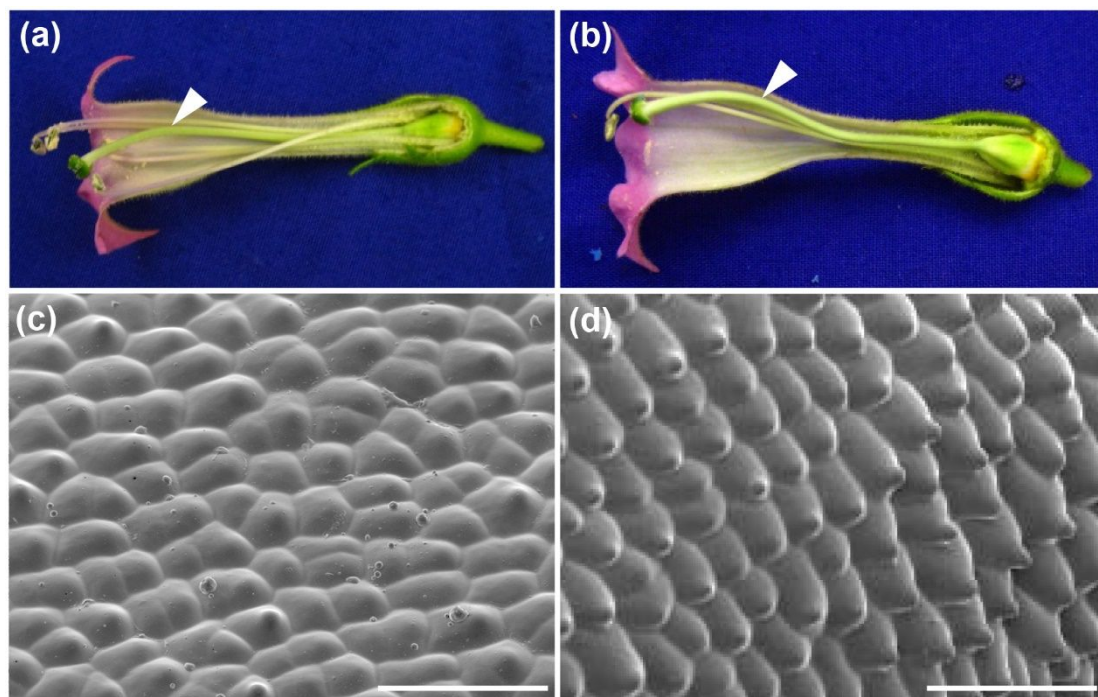
906 **Fig. 4** Drought tolerance of WT, *OX-MpSBG9*, and *mpsbg9* *M. polymorpha* plants. (a)
 907 24-day-old plants (10-day propagation of gemmae on half strength Gamborg's B5
 908 plate) were left without watering for 5 days. Scale bars, 1 mm. (b) Water content
 909 measurement of plants in (a). Each measurement represents mean \pm SE of three
 910 biological replicates. The thalli from at least 3 plants were harvested for each
 911 replicate.



912 **Fig. 5** Expression of putative *M. polymorpha* genes associated with cuticle deposition
 913 in WT, *OX-MpSBG9*, and *mpsbg9* *M. polymorpha* plants. A schematic demonstration
 914 of the cuticle biosynthesis pathway. Relative expression of putative genes orthologous
 915 to cuticle biosynthesis genes in *M. polymorpha* are displayed in the graphs. Each
 916 measurement represents mean \pm SE of three biological replicates. The thalli from at
 917 least 10 plants were harvested for each replicate. FAE, fatty acid elongase complex. *
 918 indicates no ortholog identified in *M. polymorpha*. Dashed line in gray represents
 919 plasma membrane of epidermis, with the area below the dashed line representing the
 920 extracellular space. n.d., not detected.



921 **Fig. 6** Morphology of epidermis from WT, *OX-MpSBG9*, and *mpsbg9* plants. (a-c)
 922 Dorsal view of 24-day-old plants in soil (10-day propagation of gemmae on half
 923 strength Gamborg's B5 plate), showing WT (a), *OX-MpSBG9-1* (b), and *mpsbg9-1*(c).
 924 (d-f) Cryo-SEM images of young tissues located close to the apical notch, indicated
 925 respectively by red box in (a-c). Insert in (d-f) is close-up view of papillate. (g-i)
 926 Cryo-SEM images of mature tissue at the base of thallus, indicated by black box
 927 respectively in (a-c). (j) The density of papillate in WT, *OX-MpSBG9*, and *mpsbg9*
 928 plants. Each calculation represents mean \pm SE of three biological replicates. The thalli
 929 from 3 plants were randomly collected for each replicate. (K) Size of epidermal cells
 930 in WT, *OX-MpSBG9*, and *mpsbg9* plants. Each measurement represents mean \pm SE of
 931 three biological replicates. At least fifty epidermal cells were randomly selected for
 932 each replicate. Scale bars, 1 cm in (a-c), 100 μ m in (d-i); and 50 μ m in insert of (d-f).
 933 ** $P < 0.01$ (Welch's *t* test). All comparisons were performed against WT.



934 **Fig. 7** Ectopic expression of the *MpSBG9* gene in tobacco. (a-b) Longitudinal tobacco
 935 flower dissections of WT (a) and *MpSBG9* expressing plants (b). A slight curve in the
 936 style (arrowhead) in (b) versus a fairly straight style of WT (arrowhead) in (a). (c-d)
 937 Cryo-SEM images of ovary abaxial epidermis from WT (c) and *MpSBG9* expressing
 938 plants (d). Epidermal cells range from flat to gently rounded in shape (c). Epidermal
 939 cells are relatively uniformly conical shapes in the transgenic lines (d). Scale bars,
 940 100 μm .

941 **Supporting Information**

942

943 **Fig. S1** Phylogeny of R2R3 MYB proteins.

944

945 **Fig. S2** Schematic diagram of plasmids used for *M. polymorpha* transformation.

946

947 **Fig. S3** Generation and identification of *mpsbg9* mutant *M. polymorpha* plants.

948

949 **Fig. S4** Phenotype of WT and *mpsbg9* mutant *M. polymorpha* plants.

950

951 **Fig. S5** Identification of transgenic *M. polymorpha* plants ectopically overexpressing
952 the *MpMIXTA* gene.

953

954 **Fig. S6** Epidermal morphology of WT, *OX-MpSBG9*, and *mpsbg9* *M. polymorpha*
955 plants.

956

957 **Fig. S7** Characterisation of tobacco plants constitutively overexpressing the *MpSBG9*
958 gene.

959

960 **Methods S1** Plasmid construction and plant transformation.

961

962 **Methods S2** RNA-seq analysis.

963

964 **Table S1** Transcripts with increased expression in *M. polymorpha* overexpressing
965 *MpSBG9*.

966

967 **Table S2** Transcripts with decreased expression in *M. polymorpha* *mpsbg9* mutant.

968

969 **Table S3** Top 40 transcripts with decreased expression in *M. polymorpha* *mpsbg9*
970 mutant.

971

972 **Table S4** Putative genes in *M. polymorpha* orthologous to well-know cuticle

973 biosynthesis genes in *A. thaliana*.

974

975 **Table S5** Digital gene expression.

976

977 **Table S6** Oligo primers used in this studies.

978

979 **Table S7** Raw counts. WT, wild type. OX, *OX-MpSBG9-1*. KO, *mpsbg9-1*.

For Peer Review